THE PUBLISHING HOUSE
OF THE ROMANIAN ACADEMY

PROCEEDINGS OF THE ROMANIAN ACADEMY, Series A,
Volume 27, Number 1/2026, pp. 79–88
DOI:

TRANSVERSE VERSUS AXIALLY LAMINATED ROTOR RELUCTANCE SYNCHRONOUS MOTOR FOR POWER TRAINS

Ileana TORAC[1], Lucian TUTELEA[2,1], Ion BOLDEA[2,1]

[1] Romanian Academy Timisoara Branch
[2] "Politehnica" University Timisoara
Corresponding author: Ileana TORAC, E-mail: ileana_torac@yahoo.com

Abstract. The paper presents a higher magnetic saliency-with open rotor flux barriers solution for a four-pole reluctance synchronous machine with transversal laminations anisotropic rotor. The rotor structure is very close to the axially laminated anisotropic rotor, but the manufacturing costs are estimated lower. Key FEM characterization and results for the two proposed solutions are compared in order to evaluate the applicability for power trains.

Keywords: synchronous reluctance machine, axially-laminated rotor, transverse-laminated rotor, variable speed drives, traction applications rotor.

1. INTRODUCTION

The axially laminated anisotropic (ALA) rotor reluctance synchronous machine (RSM) has a few well-known significant advantages as: no rotor winding (that means both robustness and less operating/repairing cost), a high saliency, ideally zero rotor losses and good performance (power factor ×efficiency), moderate material costs (PMs) and no problem with rotor cooling, even though for moderate torque density [1,2]. The magnetic dissymmetry of the ALA rotor is provided by a special configuration: each pole is built from grain-oriented steel laminations alternating with insulation non-magnetic material. The fastening is realized with clamping plates and screws from non-magnetic material (brass or non-magnetic stainless steel). That implies to cut each lamination and insulation sheet and then to join them in order to realize each pole (or pole pair in case of two-pole machine). Many details concerning the fabrication of an axially laminated rotor machine are presented, for a 6-pole machine, in [3]. This is the reason that, despite of the undisputable advantages of ALA rotor SRM, the machine manufacturer's objection is related to the new technology required for the fabrication of axially laminated anisotropic rotor and, consequently, unpredictable high costs; meanwhile transversely laminated rotor fabrication uses common, existing procedures, at significantly lower cost. The aim of the paper is to verify if a transversal lamination anisotropic (TLA) rotor, with open at airgap "slots" which "mimes" an axially lamination anisotropic one, could provide similar performance (for same stator data) in case of a four-pole machine of 140kW, 1900rpm, for variable speed applications. As ALA rotor SRM it produced now only as a prototype, for research purposes, the fabrication cost overcomes that of TLA rotor, which is supposed/assumed to be similar to that of induction machine rotor. For a small power six pole machine, such an investigation is presented in [3]. The paper proposes a rotor structure with a high saliency and presents key FEM validation in terms of torque and power production at base and maximum speed, d-q flux linkages and power factor in comparison with those of ALA-rotor RSM. As Ref [4] comprehensive study of TLA RSM for traction ended up with low power factor, this paper which builds up on a previous Conference paper [5] provides the following distinct new contributions: *it calculates by 2D FEM the rather complete performance at three critical operation points-max torque (1100Nm) at 610rpm, rated torque at 1900rpm and max speed 4200rpm torque (250Nm); *it demonstrates that even a 5mm wide magnetic radial rib/bridge in the TLA anisotropic rotor does not lead to notably lower performance, for power factor notably above 0.7, which reduces the burden on the inverter losses, ratings and costs; *investigation of max torque at 610rpm and

4200rpm max speed torque as typically needed in power trains; *it provides a cost comparison between the ALA and TLA rotor RSM designs. The paper continues as follows: design and data details on stator and rotor geometry in Chapter 2, key FEM electromagnetic validations in Chapter 3, Cost estimations in Chapter 4 and Conclusions in Chapter 5.

2. DESIGN DATA

The analytical preliminary design is based on previous experience and starts from the performance requirements and constraints concerning geometrical dimensions/limits.

2.1. General data

The rated power P_b=140kW, base speed n_b=1900rpm; the max. speed n_{max}=4200rpm; the outer stator diameter: DSO=389mm; the inner stator diameter DSI=245mm; the pole number 2p=4; the air gap: g=1mm; the inner rotor diameter (shaft); IRD=82mm; the dc voltage V_{dc}=600V.

2.2. Stator geometry

The core length is l_{stack}=270mm, as the assumed torque density is 22.5Nm/litre. The stator design was followed as in [6], with 36slots, chorded coils (y/τ=8/9). The winding is a double layer one, with a1=4 current path and 9turns per coil. The stator slot's dimensions are presented in Fig.1. The stator core net weight is 143.46kg, the rotor core net weight is 37.5kg for ALA and 55kg for TLA and the net weight of the stator winding is 34.5kg.

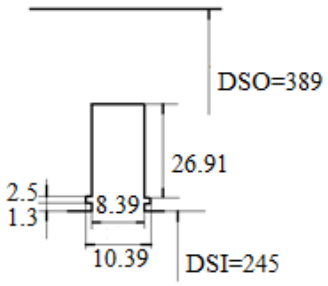

Fig. 1 – Stator slotting

2.3. TLA rotor geometry

The TLA rotor lamination is made from grain-oriented steel of 0.5mm, with 4 radial ribs and 4 spaces for fastening axial bolts, - that means a radial rib for each pole-as in Fig.2. The presence of radial ribs increases the q-axis inductance, and consequently decreases the rotor saliency, and the power factor, but is mandatory for mechanical reasons. Initially the outer diameter of the rotor lamination is the same of that of inner stator diameter, because these are cut simultaneously, So, tangential ribs (having the width resulting equal with air gap length) close the rotor barriers. The stack fastening is made with two ending nonmagnetic clamping plates and four bolts; an additional fastening is provided by a resin that fills the rotor flux barriers. The rotor final machining eliminates these tangential ribs, so the rotor barriers are open as in Fig. 2. Typical geometries of TLA with closed flux barriers are presented in [4]. As we assumed that the machine is designed for moderate speed (n_{max}=4200rpm) the rotor stack axial fastening with 4 bolts (see Fig.2) is considered a realistic, feasible solution similar with those of the stator stack fastening and does not require additional mechanical verification. The width of the radial rib of TLA is δ_{rib}, δ_{lam} is the width of the rotor lamination group and δ_{ins} is the width of the open flux barrier as in detail presented in Fig.3. The high saliency is provided by a high ratio between the pole pitch and the air gap length and also by the ratio of rotor flux barrier width/lamination group width.

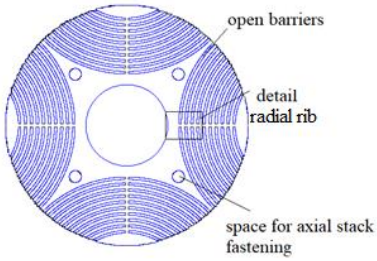

Fig. 2 – The TLA rotor cross section.

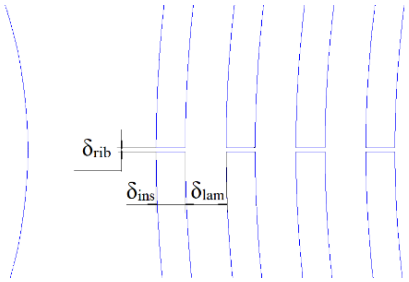

Fig. 3 – Detail of TLA rotor lamination cross section.

As q-axis space flux harmonics produce significant eddy currents in the rotor laminations, a solution to reduce core losses and also torque ripples, is to make the rotor from segments, circumferentially shifted with an equivalent total skewing of one stator slot pitch [5,6].

3. KEY FEM ELECTROMAGNETIC VALIDATIONS

The ALA rotor providing a competitive solution for the required specification is simulated in case of groups of 10 laminations/insulations, that means δ_{lam}=3.5mm, δ_{ins}=2.5mm [5]. For TLA rotor, FEM investigations were made assuming 4 values of the radial rib: δ_{rib}=[0.3; 2; 3; 5]mm. As mentioned before, the radial ribs have only a mechanical role, especially during the stack fastening, until the rotor barriers are filled with resin. So, one assumes that for δ_{rib}=0.3mm as a minimum acceptable value, one obtains the best performance for TLA rotor. Depending on the manufacturer's technology, δ_{rib}=2mm could be a feasible, realistic solution; the other values up to δ_{rib}=5mm are investigated to estimate the worsening of TLA rotor RSM performance.

3.1. Base torque point: I=263A(RMS) at base speed n_b=1900rpm

The main results are synthetized in Table 1. The estimated efficiency is 0.9442 for ALA rotor and 0.9411 for TLA rotor; the difference is due to rotor iron losses as for the same stator only the rotor structure contains more laminations. The iron losses are assumed the same for all considered δ_{rib} values (as for δ_{rib}=5mm).

Table 1

Performance at base speed (1900rpm):

	ALA	**TLA δ_{rib} [mm]**			
		0.3	**2**	**3.5**	**5**
Bm1s[T]	**0.9702**	1.0583	1.0539	1.0494	1.0494
Te[Nm]	**708.76**	748	726.71	708.19	693.36
Ld[H]	**0.0013**	0.0014	0.0013	0.0013	0.0013
Lq[H]×10^{-4}	**1.3125**	1.6962	1.8722	2.0180	2.1531
Ld/Lq	**9.705**	7.94	7.1167	6.53	6.0775
Ψd[Wb]	**0.7859**	0.8469	0.8378	0.8289	0.8228
Ψq[Wb]	**0.1737**	0.2287	0.2524	0.2721	0.2903
Ψs[Wb]	**0.89**	0.8773	0.875	0.8724	0.8725
Id[A]	**157.212**				
Iq[A]	**337.0772**				
cosφ ideal	**0.7937**	0.7647	0.7458	0.7292	0.714
cosφ	**0.8223**	0.7970	0.7794	0.7518	0.7511
η[%]	**0.9442**				0.9411
Vs[V](RMS)	**327.23**	355.78	354.73	353.56	353.47
Pe[kW]	**137.96**	148.83	144.59	140.91	141.02

The FEM obtained ideal power factor is:

$$\cos\varphi = \cos\left(\tan^{-1}\left(\Psi_q/\Psi_d\right) + \tan^{-1}\left(I_d/I_q\right)\right) \quad (1)$$

With the copper losses included, the power factor is obtained as follows:

$$\cos\varphi = \cos\left(\tan^{-1}\left[\omega_1\left(L_d i_d^2 + L_q i_q^2\right)\right] / \left[\omega_1\left(L_d - L_q\right) i_d i_q + R_s\left(i_d^2 + i_q^2\right)\right]\right) \quad (2)$$

The efficiency was calculated considering the copper losses from FEM simulations; iron losses and mechanical losses were calculated as in [7]. **Note**: We assumed that for TLA rotor the laminations are cut by the standard, common procedure, as for stator laminations. In case of other procedures (as laser cutting) required by other different rotor configurations, the degradation of the core magnetic proprieties on material edges could modify notably the iron losses value [8]. Table 2 emphasizes the parameters modification of RSM with TLA rotor, with respect to those of RSM with ALA rotor.

Table 2

Performance difference at base speed (1900rpm):

	ALA	**TLA vs ALA parameter modification [%] for different values of δ_{rib} [mm]**			
		0.3	**2**	**3.5**	**5**
Te[Nm]	**708.76**	+5.53	+2.53	–0.08	**–2.17**
Ld/Lq	**9.705**	–18.18	–26.67	–32.72	**–37.38**
cosφ ideal	**0.7937**	–3.65	–6.03	–8.13	**–10.04**
cosφ	**0.8223**	–3.07	–5.21	–8.57	**–8.65**
η[%]	**0.9442**				**–3.28**

The FEM simulations results for rotor structure with δ_{rib}=5mm are presented below. The no-load air gap flux density fundamental and the flux density distribution on the TLA rotor machine cross section are presented in Fig.4,5 for Id=157.212A(peak), which is the phase current assumed for peak torque.

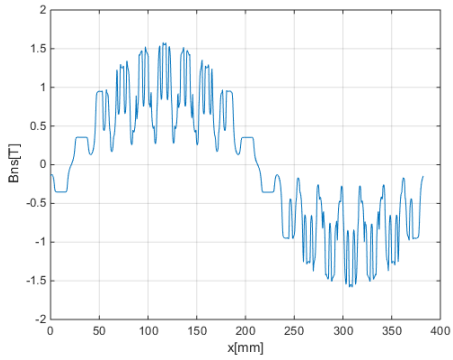

Fig. 4 – The air gap flux density for TLA rotor machine with δrib=5mm, in axis d for Id=157.212A(peak), Iq=0.

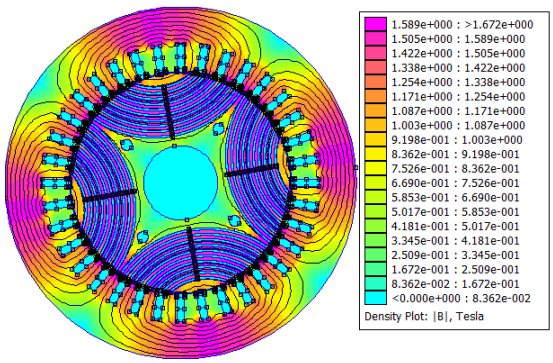

Fig. 5 – The flux density distribution in axis d on the TLA machine cross section for Id=157.212A(peak), Iq=0. (δrib=5mm)

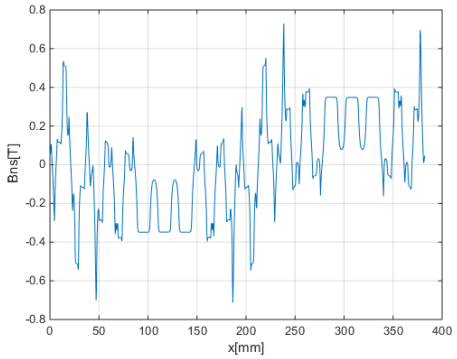

Fig. 6 – The air gap flux density for TLA rotor machine (δrib=5mm), in axis q for Iq=337.0772A(peak), Id=0.

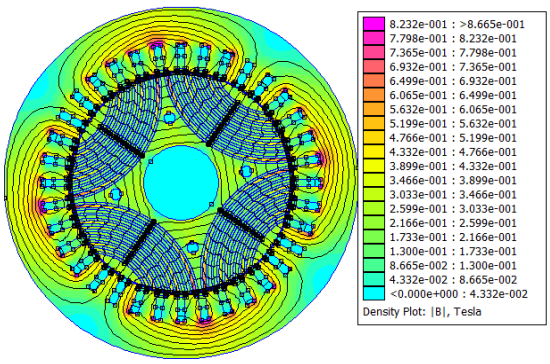

Fig. 7 – The flux density distribution on TLA rotor machine cross section (δrib=5mm), for Iq=337.0772A(peak), Id=0.

The fundamental of no-load air gap flux density is B_{1d0}=1.065T. The air gap flux density distribution and the flux density distribution on the machine cross section (in case of TLA rotor) for q-axis (Id=0), are presented in Fig 6,7 for Iq=337.0772A(peak) which is the phase current assumed for peak torque.

The fundamental of q-axis air gap flux density is B_{1q0}=0.2379T, with a high content of harmonics. The air gap flux density distribution for rated torque, I_d=157.212A(peak), I_q=337.0772A(peak), current angle 57.5° (Is=263A(RMS), base speed) are shown in Fig8 for ALA rotor machine and in Fig 9 for TLA rotor machine with δ_{rib}=5mm.

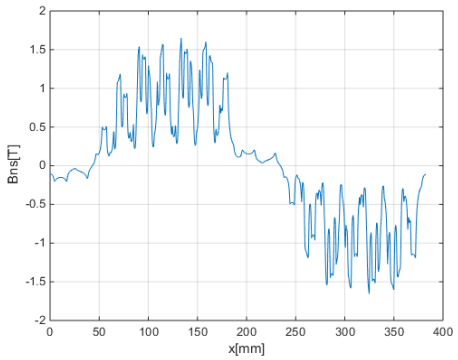

Fig. 8 – The air gap flux density distribution for rated torque, Id=157.212A(peak), Iq=337.0772A(peak), current angle 57.5°, (Is=263A(RMS), base speed) for ALA rotor machine.

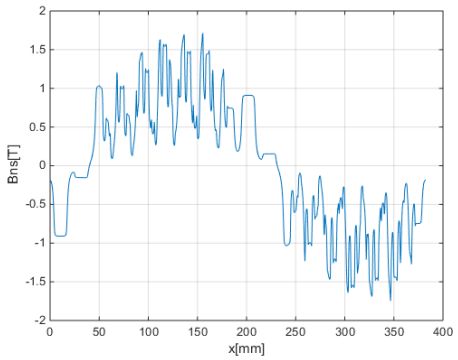

Fig. 9 – The air gap flux density distribution for rated torque, Id=157.212A(peak), Iq=337.0772A(peak), current angle 57.5°, (Is=263A(RMS), base speed) for TLA rotor machine.

For TLA rotor machine, the flux density distribution on machine cross section is presented in Fig. 10 and the d and q-axis flux linkages depending upon the rotor position are presented in Fig. 11. The average value of d and q-axis fluxes are Ψd=0.8228Wb, Ψq=0.2903Wb, so, Ψd/Ψq=2.8343(for TLA rotor).

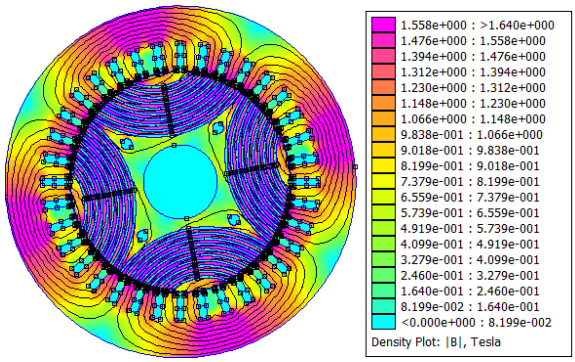

Fig. 10 – The flux density distribution on TLA rotor machine cross section (δrib=5mm), for rated torque, Id=157.212A(peak), Iq=337.0772A(peak), current angle 57.5°, (Is=263A(RMS), base speed).

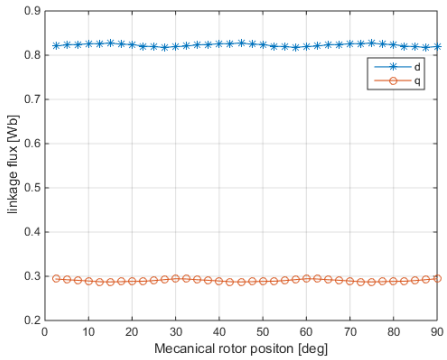

Fig. 11 – The TLA machine d and q-axis linkage flux for rated torque, Id=157.212A(peak), Iq=337.0772A(peak), current angle 57.5°, (Is=263A(RMS), base speed), (δrib=5mm).

The machine torque for Is=263A(RMS) depending on the mechanical rotor position, for a straight rotor (Te) and for a three segments rotor (Tm), with a total skewing of one stator slot pitch is shown in Fig 12 for ALA rotor and in Fig. 13 for TLA rotor with δ_{rib}=5mm.

The average value is practically the same, but in case of segmented rotor the torque ripples are reduced from 11% to 4.34% in case of ALA rotor and from 11.5% to 4.5% for TLA rotor (peak to peak value).

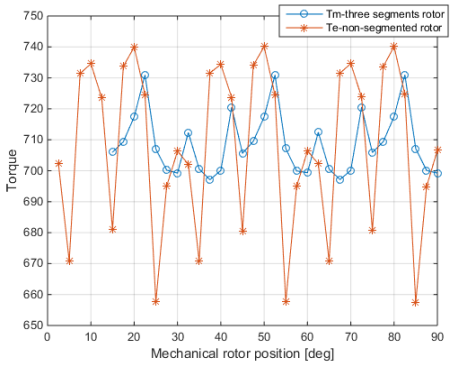

Fig. 12 – The machine torque (in Nm) for Is=263A(RMS)current angle 57.5°, for non-segmented rotor (Te) and for a three segments rotor (Tm) for ALA rotor.

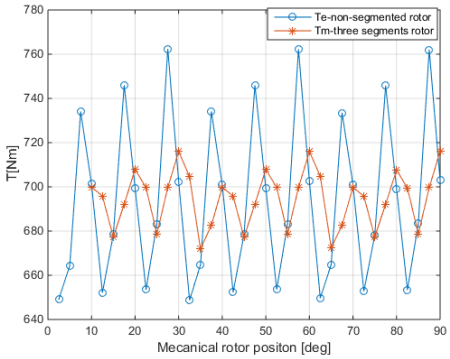

Fig. 13 – The machine torque (in Nm) for Is=263A(RMS)current angle 57.5°, for non-segmented rotor (Te) and for a three segments rotor (Tm) for TLA rotor.

3.2. Max torque point: I=385A(RMS) at T=1100Nm, n=610rpm

For the max torque operating regime, I=385A(RMS), n=610rpm, one obtains 70kW. The flux density distribution in the machine cross section for peak torque currents Id=186.188A(peak), Iq=511.6(peak), current angle 55° are shown in Fig. 14 for ALA rotor composed from groups of 10laminations/insulations, (that means δ_{lam}=3.5mm, δ_{ins}=2.5mm) and in Fig. 15 for TLA rotor with δ_{rib}=5mm. One emphasizes a higher saturation level in case of TLA rotor which explains a small decrease of the power factor. The results are presented in Table 3 and the performance comparison in Table 4. The estimated efficiency is 0.8458 for ALA rotor and 0.8527 for TLA rotor as the obtained torque is with +5.77% larger for TLA rotor.

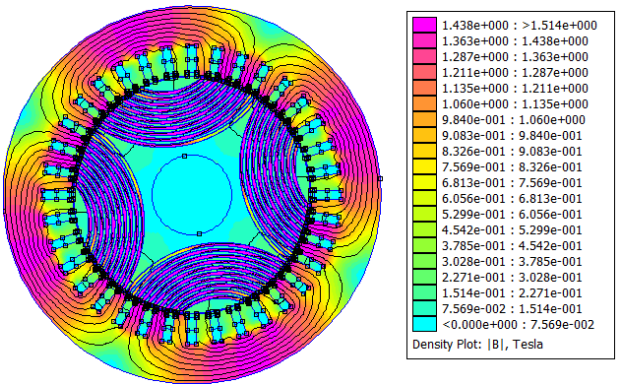

Fig. 14 – The flux density distribution on ALA rotor machine cross section, for max torque, Id=186.188A(peak), Iq=511.6A(peak), current angle 55°, (Is=385A(RMS), n=610rpm).

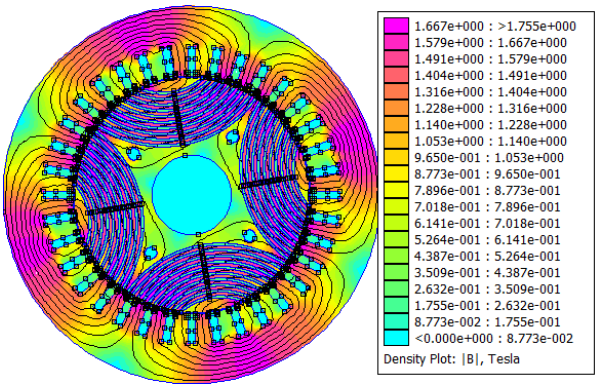

Fig. 15 – The flux density distribution on TLA rotor machine cross section (δrib=5mm), for max torque, Id=186.188A(peak), Iq=511.6A(peak), current angle 55°, (Is=385A(RMS), n=610rpm).

The machine torque for Is=385A(RMS), current angle 55° depending on mechanical rotor position for a straight rotor (Te) and for a three segments rotor (Tm), with a total skewing of one stator slot pitch is shown in Fig 16 for ALA rotor and in Fig. 17 for TLA rotor with δ_{rib}=5mm. In case of segmented rotor, the torque ripples are reduced from 11.33% to 4.47% for ALA and from 12.2% to 4.87% for TLA (peak to peak value). In case of max torque, one finds slightly better results in terms of torque and efficiency for TLA rotor machine in comparison with ALA rotor SRM (Table 4).

Table 3

Performance for max torque=1100Nm, n=610rpm

	ALA	**TLA δ_{rib} =5[mm]**
Bm1s[T]	**1.0056**	1.1108
Te[Nm]	**1084**	1146.6
Ld[H]	**0.0013**	0.0012
Lq[H]×10^{-4}	**1.25**	1.6606
Ld/Lq	**8.52**	7.04
Ψd[Wb]	**0.8054**	0.8706
Ψq[Wb]	**0.2597**	0.3399
Ψs[Wb]	**0.8463**	0.9345
Id[A]	**186.188**	
Iq[A]	**511.6**	
cosφ ideal	**0.7894**	0.751
cosφ	**0.8959**	0.8607
η[%]	**0.8458**	0.8527
Vs[V](RMS)	**118.42**	129.24
Pe[kW]	**69.245**	73.244

Table 4

Performance difference for max torque=1100Nm, n=610rpm

	ALA	**TLA vs ALA modification [%] δ_{rib} =5[mm]**
Te[Nm]	1084	+5.77
Ld/Lq	8.52	–17.37
cosφ ideal	0.7894	–4.86
cosφ	0.8959	–3.93
η[%]	0.8458	+0.85

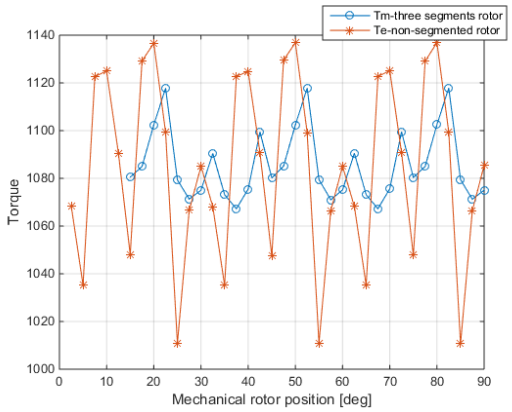

Fig. 16 – The machine torque (in Nm) for Id=186.188A(peak), Iq=511.6A(peak), current angle 55°, (Is=385A(RMS), for non-segmented rotor (Te) and for a three segments rotor (Tm) for ALA rotor.

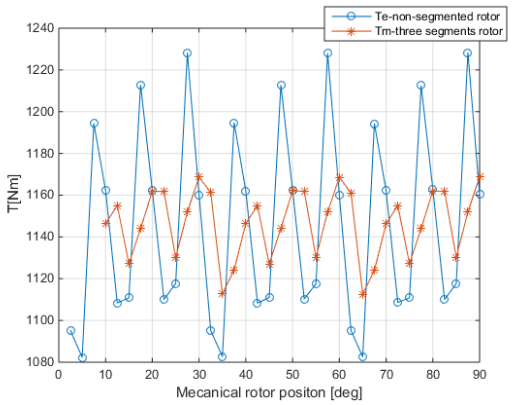

Fig. 17–The machine torque (in Nm) for Id=186.188A(peak), Iq=511.6A(peak), current angle 55°, (Is=385A(RMS), for non-segmented rotor (Te) and for a three segments rotor (Tm) for TLA rotor (δrib=5mm).

3.3. Max speed point: I=167A(RMS) at max. speed n_{max}=4200rpm

The air gap flux density distribution and the flux density distribution in the machine cross section with TLA rotor for Is=167A(RMS), that means Id=53.1072A(peak), Iq=230.12A(peak), current angle 51.5° for maximum available voltage (as in Table 5) are shown in Fig. 18 and Fig. 19 respectively.

At max speed the results are presented in Table 5 and the performance differences in Table 6.

The estimated efficiency is 0.9389 for ALA rotor and 0.9377 for TLA rotor. The machine torque for max speed, Is=167A(RMS) current angle 51.5° as function upon the mechanical rotor position, for a straight rotor (Te) and for a considered three segment rotor (Tm) with a total skewing of one stator slot pitch is shown in Fig. 20 for ALA rotor and in Fig.21 for TLA rotor machine. In case of segmented rotor, the torque ripple is reduced from 28% to 10% in first case and from 15.14% to 5.58% in the second one (peak value). Also, for max speed one finds slightly better torque (with a -0.12% efficiency) for TLA rotor machine in comparison with ALA rotor SRM.

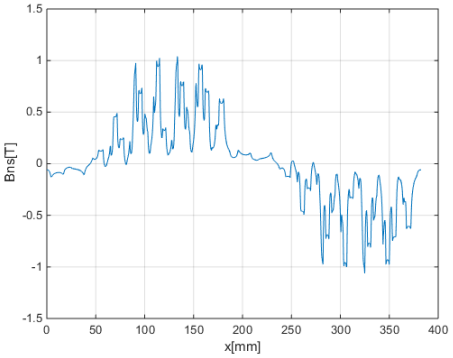

Fig. 18 – The air gap flux density distribution for max speed, n=4200rpm, Id=53.1072A(peak), Iq=230.12A(peak), current angle 51.5°, (Is=167A(RMS), base speed) for TLA rotor machine (δrib=5mm).

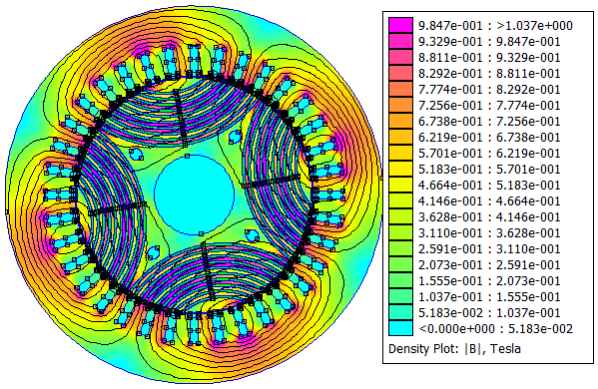

Fig. 19 –The flux density distribution on the machine cross section for max speed, n=4200rpm, Id=53.1072A(peak), Iq=230.12A(peak), current angle 51.5°, (Is=167A(RMS), base speed) for TLA rotor machine (δrib=5mm).

Table 5

Performance for max speed, n=4200rpm

	ALA	**TLA δ_{rib} =5[mm]**
Bm1s[T]	**0.4783**	0.5221
Te[Nm]	**238**	251
Ld[H]	**0.0018**	0.0019
Lq[H]×10^{-4}	**1.4269**	1.8076
Ld/Lq	**12.5**	10.477
Ψd[Wb]	**0.3789**	0.4022
Ψq[Wb]	**0.1313**	0.1664
Ψs[Wb]	**0.401**	0.4353
Id[A]	**53.1072**	
Iq[A]	**230.12**	
cosφ ideal	**0.847**	0.8144
cosφ	**0.8647**	0.8353
η[%]	**0.9389**	0.9377
Vs[V](RMS)	**357.43**	387.39
Pe[kW]	**52.339**	55.198

Table 6

Performance difference for max speed, n=4200rpm

	ALA	**TLA vs ALA modification [%] δ_{rib} =5[mm]**
Te[Nm]	238	+5.46
Ld/Lq	12.5	–16.84
cosφ ideal	0. 847	–3.85
cosφ	0.8647	–3.4
η[%]	0.9389	–0.12

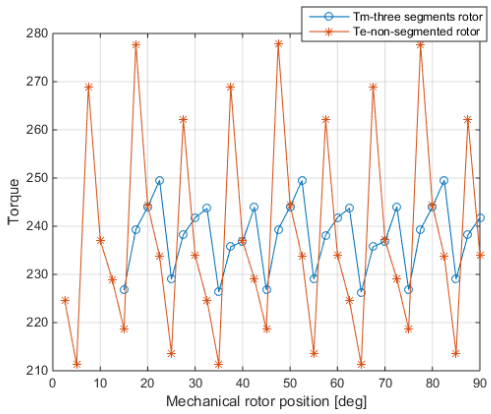

Fig. 20 – The machine torque (in Nm) for Id=53.1072A(peak), Iq=230.12A(peak), current angle 51.5°, (Is=167A(RMS), for non-segmented rotor (Te) and for a three segments rotor (Tm) for ALA rotor.

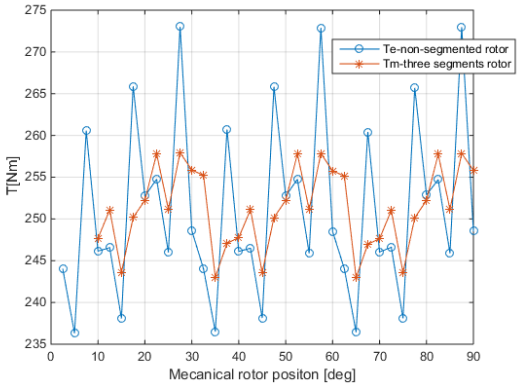

Fig. 21–The machine torque (in Nm) for Id=53.1072A(peak), Iq=230.12A(peak), current angle 51.5°, (Is=167A(RMS), for non-segmented rotor (Te) and for a three segments rotor (Tm) for TLA rotor (δrib=5mm).

1.4. Summary of FEM electromagnetic validations

Table 7 summarizes the main results of FEM characterization of the two solutions for the three critical operating points. It shows that in term of energy conversion TLA rotor, in the considered configuration, almost globally matches the ALA rotor configuration, for a simple rotor fabrication technology.

Table 7

Synthetic performance in 3 crucial operating points

	Max torque point		**Rated torque point**		**Max speed**	
	ALA	**TLA**	**ALA**	**TLA**	**ALA**	**TLA**
Te[Nm]	1084	1146.6	708.76	693.36	238	251
n[rpm]	610		1900		4200	
Is[A] (RMS)	385		263		167	
Current angle	57.5°		55°		51.5°	
cosφ ideal	0.7894	0.751	0.7937	0.714	0.847	0.8144
cosφ	0.8959	0.8607	0.8223	0.7511	0.8647	0.8353
η[%]	0.8458	0.8527	0.9442	0.9411	0.9389	0.9377
Vs[V](RMS)	118.42	129.24	327.23	353.47	357.43	387.39
Pe[kW]	69.245	73.244	137.96	141.02	52.339	55.198

4. COST ESTIMATION

A realistic estimation of costs refers to active materials (iron, copper), auxiliary materials (frame, shields, etc), fabrication cost and converter price. ALA and TLA rotor SRM have the same stator; the rotor volume is the same for both topologies. One the other side, an honest, realistic material cost estimation has to consider the whole quantity of materials (that means including the technological losses). For ALA rotor, the fabrication is in the prototyping stage. TLA rotor fabrication is similar with that of induction machine rotor because the laminations stack fastening is a common, standard procedure. The filling of rotor flux barriers with resin is also a standard, unexpensive procedure. The converter choosing is based on peak current (corresponding to max torque point) and on the peak voltage (corresponding to the max speed point) as they are in Table 8; so, the inverter required power is S=450kVA. For both ALA and TLA rotor solutions the same converter is basically needed.

Table 8

Synthetic data for converter requirements

	Max torque point		**Rated torque point**		**Max speed**	
	ALA	**TLA**	**ALA**	**TLA**	**ALA**	**TLA**
Te[Nm]	1084	1146.6	708.76	693.36	238	251
n[rpm]	610		1900		4200	
Is[A] (peak)	**544.4**7		371.9382		236.1737	
Vs[V](RMS)	167.47	182.77	462.77	499.88.	505.48	**547.85**

One assumes the cost of auxiliary components is 60% from the cost of the active materials. For the fabrication cost, one assumes as being 1.15 times of active materials cost for TLA (as for induction machine) and 1.3 times for ALA, respectively. The assumed price is 10EUR for copper and 3.5EUR for lamination steel (iron). For the inverter one considers 20EUR per KVA.

The estimated total (drive) cost including the inverter is 13,335EUR for ALA rotor and 13,111EUR for TLA rotor SRM, so one can conclude that the later one is less expensive in comparison with ALA rotor machine.

Table 9

Cost synopsis for the proposed solutions

	ALA		**TLA**	
	weight [kq]	Cost [EUR]	weight [kq]	Cost [EUR]
Copper	37.5	375	37.5	375
Iron (laminations)	320	1120	320	1120
Active materials	-	1495	-	1495
Auxiliary materials	-	897	-	897
Fabrication	-	1943	-	1719
Machine		**4335**		**4111**
Converter	-	**9000**	-	**9000**
Total	-	**13,355**		**13,111**

5. CONCLUSION

The paper proposes a solution for a motor of 140kW, 1900-4200rpm with transverse laminations anisotropic (TLA) rotor with open flux barriers, introduced to reduce rotor cost fabrication with respect to ALA rotor (but providing practically the same rotor anisotropy). The proposed configuration applicable for moderate speeds, could be realized with existing, standard, unexpensive technologies, in comparison with other proposed topologies [8] for high speeds that require additional investigations about manufacturing stresses on machine performance. The key FEM validation results confirm the proposed solution, in sense of producing about the same average torque as ALA rotor at same Id and Iq: at base speed for a 7.38A/mm^2; at max torque, at speed n=610rpm for a 10.85A/mm^2; the same was found valid for max speed torque at about same efficiency. However, for a more complete solution assessment, further in-depth FEM investigation for a given operating regime regarding thermal and mechanical stresses, optimal design, prototyping and testing are due in the future. The difference between FEM simulation results and measured values of the machine performance could be up to 3-5% so FEM is assumed as a thrusted reliable modelling methodology before the prototyping manufacture.

REFERENCES

[1] Boldea I. Reluctance synchronous machine and drives, book, Oxford UP, England,1996.
[2] Boldea I., Tutelea L. Reluctance electric machines design and control, book, CRC Press, 2021.
[3] Agamloch E, Deb S. Performance comparison of transverse and axially laminated synchronous machines, 2022 IEEE Energy Convention Congress and Exposition (ECCE), DOI: 10.1109/ECCE50734.2022.9947590.
[4] Credo A, Fabri G., Villani, M., Popescu M Adopting the topology optimization on the design of high-speed synchronous reluctance motors for electric vehicles, IEEE Trans. Vol. IA-56, no5, 2020, pages 5429-5438. DOI: 10.1109/TIA.2020.3007366.
[5] Torac I., Tutelea L., Boldea I. Transverse versus axially-laminated rotor RSM: key FEM validation, 2025 International Aegean Conference on Electrical Machines and Power Electronics (ACEMP) &International Conference on Optimization of Electrical and Electronic Equipment (OPTIM) 2025 DOI: 10.1109/OPTIM-ACEMP62776.2025.11075266.
[6] Boldea I., Torac I., Tutelea L. 100kW 6-12krpm ALA rotor traction motor: preliminary design with key electromagnetic FEM validation, IEEE EUROCON 2023-20th International Conference on Smart Technologies Italy, Torino, 2023. DOI: 101109/EUROCON56442.2023.10199033.
[7] Richter R. Kurz Lehrbuch der Elektrische Maschinen, Springer Verlag, Berlin, 1949.
[8] Credo A. Petrov I., Pyrhönen Villani M. Impact of Manufacturing Stresses On Multiple-Rib Synchronous Reluctance Motor Performance, IEEE Transactions On Industry Applications, vol 59, NO2, MARCH/APRIL, 2023, pag.1253-1262, DOI: 10.1109/TIA.2022.3207117.

Received February 11, 2026